Photodissociation Dynamics of 4-Aminobenzonitrile$^+$(Water)$_n$ Clusters

Mi Ae Lee, Sang Hwan Nam, Hye Sun Park, Nu Ri Cheong, Seol Ryu, Jae Kyu Song,* and Seung Min Park*

Department of Chemistry, Kyunghee University, Seoul 130-701, Korea
**E-mail: jaeksong@khu.ac.kr (J. K. Song); smpark@khu.ac.kr (S. M. Park)*
Received October 6, 2008

The photodissociation dynamics of 4-aminobenzonitrile$^+$(water)$_n$ (4ABN$^+$W$_n$) (n = 1-18) clusters was investigated using a home-built linear-tandem time-of-flight (TOF) mass spectrometer consisting of two stages. Mass-selected cluster cations (n = 8-18) were irradiated by photons with energies ranging from 2.15 to 2.95 eV in the field-free region at the second stage. The average numbers of ejected water molecules were obtained at various photon energies from the photofragmentation mass spectra, from which the average binding energies of water molecules were estimated. Also, the optimum structures of the clusters and binding energies of the water molecules were suggested *via* theoretical calculations. The local excitation (LE) band observed in the photodissociation spectra of the 4ABN$^+$W$_n$ (n = 1-3) clusters and 4ABN$_2^-$ shifted to blue with increase in the number of solvated water molecules.

Key Words : Photodissociation, Cluster, Binding energy

Introduction

The photodissociation of size-selected cluster ions has been widely examined to understand energy transfer processes in clusters and to elucidate their structures.[1-11] In particular, photofragmentation of electronically excited aniline$^-$(water)$_n$ (An$^+$W$_n$) clusters has been recently investigated to shed light on the intermolecular interaction between the amino group and water in the ionic state, where the average binding energies of water molecules with n = 5-20 were obtained and the optimized structures with n = 1-7 were suggested from the density functional theory (DFT) calculations.[11]

Here, we adopt 4-aminobenzonitrile$^+$(water)$_n$ (4ABN$^-$W$_n$) clusters to verify the effects of cyano group on the structures and binding energies compared to An$^+$W$_n$ clusters. Namely, while aniline has only one binding site (amino), 4ABN has two: amino and cyano group.[12-15] Which site will be preferentially solvated with water? For the last 20 years, many experimental and theoretical studies on neutral 4ABN and 4ABN-W$_1$ isomers have been carried out.[12-20] For 4ABN-W$_1$, three isomer structures were identified: NH$_2$ donor, CN side, and CN linear.[12-15] The isomer of the NH$_2$ donor turned out to give the most stable structure and the neutral structure of 4ABN-W$_1$ isomers was confirmed based on laser-induced fluorescence (LIF) spectra.[13]

Also, an experimental attempt adopting pulsed field ionization zero-kinetic energy photoelectron spectroscopy was performed to acquire stable structures for 4ABN$^+$W$_1$.[15] When the number of solvated water molecules is small, the water molecules are expected to be bound mostly at the NH$_2$ site as in the case of the An$^+$W$_n$ cluster. However, we cannot rule out the possibility of competitive binding at CN site as the number of water molecules increases. According to our results for 4ABN$^-$W$_n$ (n = 1-7) obtained through DFT calculation, the most stable structures were obtained when the water molecules were bound at the NH$_2$ site as in the case of the An$^-$W$_n$ clusters. But the differences in the binding energy for the two sites became negligible for larger clusters with $n \geq 5$.

In the present work, the average number of ejected water molecules and the average binding energy of the water molecules have been obtained as a function of photon energy through mass-selected photofragmentation. With increasing photon energy, the average number of ejected molecules increases linearly, which conforms to our previous results on An$^-$W$_n$ clusters. Also, the binding energies of the 4ABN$^-$W$_n$ clusters were compared with those of the An$^-$W$_n$ clusters. Although there are two distinct moieties for 4ABN$^-$ ion where water molecules can be attached, the binding energies of the 4ABN$^-$W$_n$ clusters were close to those of the An$^-$W$_n$ clusters. Interestingly, the binding energy for the 4ABN$^-$W$_{14}$ cluster was prominent among clusters with $12 \leq n \leq 18$, which presumably reflects its structural stability.

Experimental

A detailed description of the experimental apparatus has been previously reported.[11,21,22] Briefly, 4ABN was heated to 90 °C in the sample oven mounted in the source chamber where water was bubbled at room temperature using inert gas as carrier. Three carrier gases (helium, argon, and xenon) were employed with a stagnation pressure of 3 atm. The gas mixture was expanded through a pulsed nozzle that was maintained at 120 °C and collimated using a skimmer. So-produced 4ABN-W$_n$ clusters were ionized at the first stage *via* two-photon ionization using the fourth harmonic output (266 nm) of a Nd:YAG laser (Spectra-Physics, GCR 150-10). An optical parametric oscillator laser (Continuum, Panther EX) pumped by the third harmonic output of a Nd:YAG laser (Continuum, Surelite III) was used to photo-

dissociate mass-selected cluster ions at the second stage. The voltages of the repeller and the extractor electrode at the first stage were 4,804 and 4,500 V, respectively. The second stage consists of four electrodes; the first and the fourth were at ground potential and 2,500 V was applied to the second and the third. Photodissociation occurs in the field-free region between the second and the third electrodes at the second stage. The parent and daughter ions generated have different kinetic energies and are distinguished as they pass the second stage after photofragmentation. The ions were detected using a microchannel plate (MCP), the signal of which was recorded using a digital storage oscilloscope (LeCroy, WaveSurfer 454) after amplification. We acquired the difference mass spectra of the fragment ions at various photon energies for $4ABN^{-}W_n$. The number of ejected water molecules was plotted as a function of the photon energy and the average binding energy was evaluated from the inverse of the slope.

Results and Discussion

Selection of a carrier gas. The TOF mass spectra of the $4ABN^{+}W_n$ cluster for different carrier gases are shown in Figure 1. In all of these spectra, not only hydrated monomer ions, $4ABN^{+}W_n$, but also hydrated dimers were detected. Also, the changes in mass distributions for the different carrier gases were highly apparent; cluster ion as large as n = 49 was observed for Ar while n = 60 cluster ion was detectable for Xe. Accordingly, the intensities for small cluster ions increased dramatically as He is used as a carrier gas. As explained by Kappes *et al.*,[23] the above results stem from two factors: one is the number of collisions and the other is the thermal accommodation coefficient. Considering the atomic weight, the mean flow velocity in a helium-seed expansion is the largest of three gases. Therefore, in He carrier gas, more cluster-gas collisions and fewer cluster-cluster collisions are predicted than in Ar and Xe. Also, the thermal accommodation coefficient increases in proportion to the atomic size of carrier gas. Hence, Xe shows the most powerful cooling effect through expansion compared to He and Ar. Consequently, relatively smaller clusters are formed in He-seed expansion as shown in Figure 1. In our experiment, Ar has been chosen as a carrier gas since it generates medium-sized clusters ($8 \le n \le 18$) in densities large enough to carry out photofragmentation experiment.

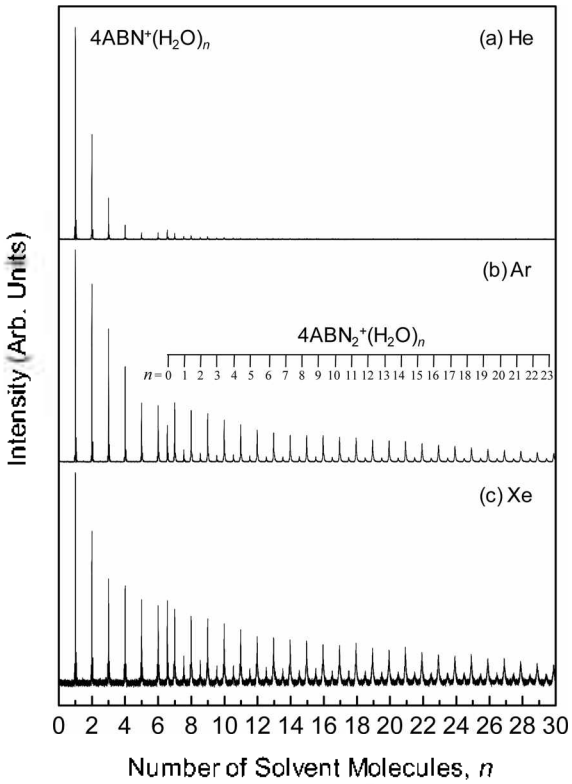

Figure 1. Photoionization mass spectra for $4ABN^{-}W_n$. The carrier gases were (a) He, (b) Ar, and (c) Xe, respectively.

Structure identification of the $4ABN^{-}W_n$ clusters. The optimized structures and binding energies of the $4ABN^{+}W_n$ (n = 1-7) clusters were calculated with the GAUSSIAN03 program package at the B3LYP/cc-pVDZ level. The most stable structures are displayed in Figure 2, and the calculated absolute energies corrected with zero-point vibrational energies are indicated in Table 1. The NH_2 donor isomer is more stable than the CN side isomer for the $4ABN^{-}W_1$ cluster and

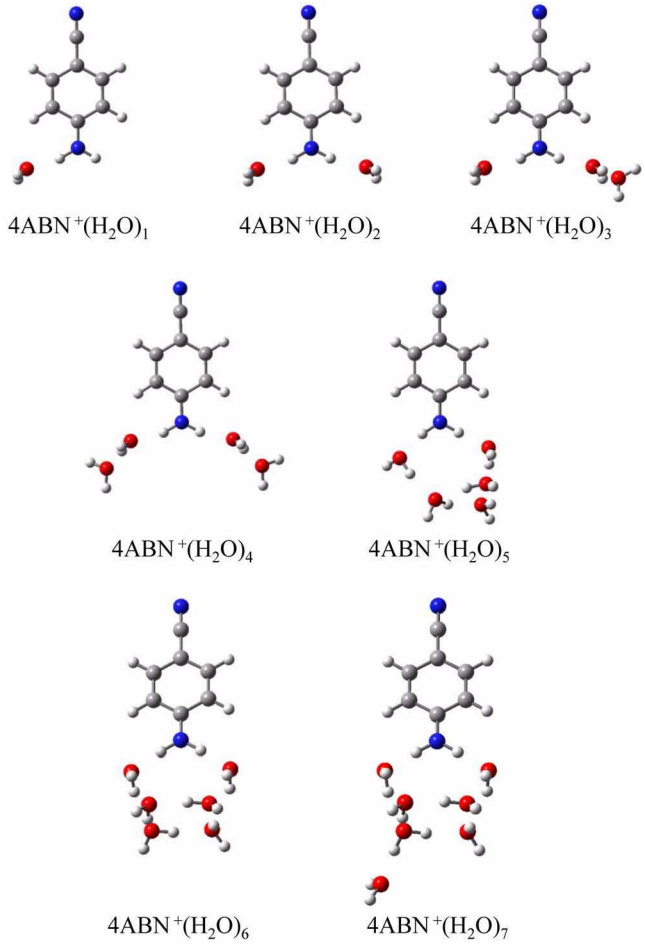

Figure 2. The optimized structures for the most stable isomers of the $4ABN^{-}W_n$ (n = 1-7) clusters.

Table 1. Absolute energies of the $4ABN^-W_n$ (n = 1-7) clusters obtained through DFT calculation

Species	E_{zpve} (hartree)
$4ABN^-$	−379.472505
H_2O	−76.399520
$4ABN^-(H_2O)_1$	−455.903356
$4ABN^-(H_2O)_2$	−532.330870
$4ABN^-(H_2O)_3$	−608.752816
$4ABN^-(H_2O)_4$	−685.173881
$4ABN^-(H_2O)_5$	−761.597734
$4ABN^-(H_2O)_6$	−838.025415
$4ABN^-(H_2O)_7$	−914.445180

Table 2. Binding energies of the $4ABN^-W_n$ and the An^-W_n (n = 1-7) clusters obtained through DFT calculation

	L = 4ABN	L = An	
$L^-(H_2O)_n \rightarrow L^-(H_2O)_{n-1} + H_2O$	E_b (eV)	E_b (eV)[a]	ΔE_b (eV)[b]
n = 1	0.8526	0.8193	+0.0333
n = 2	0.8526	0.7274	−0.0344
n = 3	0.6102	0.5875	−0.0227
n = 4	0.5863	0.5636	−0.0227
n = 5	0.6621	0.6735	−0.0114
n = 6	0.7663	0.8143	−0.0480
n = 7	0.5509	0.5397	+0.0112

[a]Reference 11. [b]E_b (eV) of the $4ABN^-(H_2O)_n$ cluster − E_b (eV) of the $An^-(H_2O)_n$ cluster.

all the larger cluster ions (n = 1-7) have similar structures to those of the corresponding An^-W_n clusters.

Table 2 shows the binding energies of the water molecules for the most stable structures of the $4ABN^-W_n$ and the An^+W_n (n = 1-7) clusters, together with the differences in the binding energies of the water molecules for the $4ABN^-W_n$ and the An^+W_n (n = 1-7) clusters. The binding energies of $4ABN^+W_n$ cluster are larger than those of the An^-W_n clusters except for n = 5, 6. The cyano group has the electron-withdrawing character, whereas the amino group has the role of proton donor. The charge of amino proton of neutral 4ABN is more positive than that of the neutral aniline because of the cyano group.[12,13] Consequently, 4ABN-W_n cluster has larger binding energies when water molecules are bound at the NH_2 site. But, in the ionic state, the charge of amino proton of 4ABN is similar to that of the aniline. Therefore, the differences in the binding energies between $4ABN^+W_n$ and An^-W_n clusters are thought to originate from the overall charge distributions including dipole and quadrupole interactions.

In neutral 4ABN-W_1 cluster, NH_2 isomer is more stable than CN isomer just by 0.0428 eV. But the difference increases up to 0.370 eV as it gets ionized. For $4ABN^+W_3$, the difference in energy between the most stable isomer with three water molecules at amino site and the isomer with two water molecules symmetrically bound to the hydrogen at NH_2 site and one water molecule at CN site down to 0.189 eV. For $4ABN^+W_7$, the difference between the most stable and the second most stable isomers reduces further down to 0.165 eV. This implies that binding of water molecules at cyano site becomes more plausible with increase in the number of water molecules.

Although the most stable structures of the $4ABN^+W_n$ clusters resemble those of the An^+W_n clusters, the differences in the binding energies for $4ABN^-W_n$ and An^-W_n are not negligible and strongly depend on the structures; for n = 5, 6, the binding energies of $4ABN^+W_n$ are smaller than those of An^+W_n, presumably due to the less significant structural stability originated from the formation of ring structures as suggested for An^-W_n.[11]

Local excitation band. The photodissociation spectra of $4ABN^-W_n$ clusters (n = 1-3) and $4ABN_2^-$ cluster in the energy range of 19,600-23,800 cm^{-1} (420-510 nm) are illustrated in Figure 3. $4ABN^-$ was the only photofragment ion detected through photodissociation and care has been taken to confirm a linear response of the fragment ion intensity over the relevant laser fluence. The positions of the local excitation (LE) bands for $4ABN^-$ turned out to shift as results of hydration or formation of a dimer: 21,046 cm^{-1}, 21,269 cm^{-1}, 21,360 cm^{-1}, and 21,224 cm^{-1} for $4ABN^-W_1$,

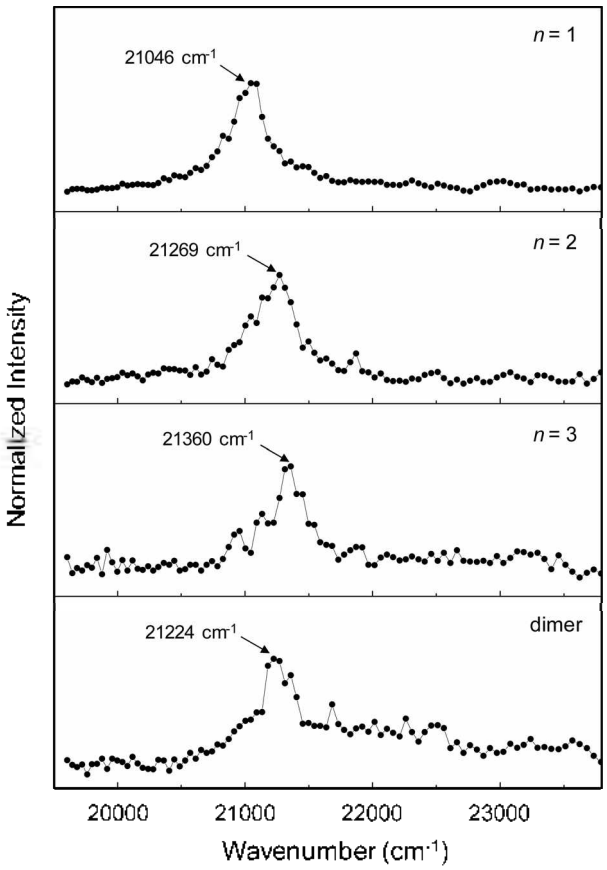

Figure 3. Photodissociation spectra of $4ABN^-W_n$ (n = 1-3) and $4ABN_2^-$ within the energy range of 19,600-23,800 cm^{-1}. The normalized yields of the fragment ion, $4ABN^-$ are plotted as a function of the wavenumber of the dissociation laser. One local excitation (LE) band is observed for all the cluster ions (carrier gas: argon).

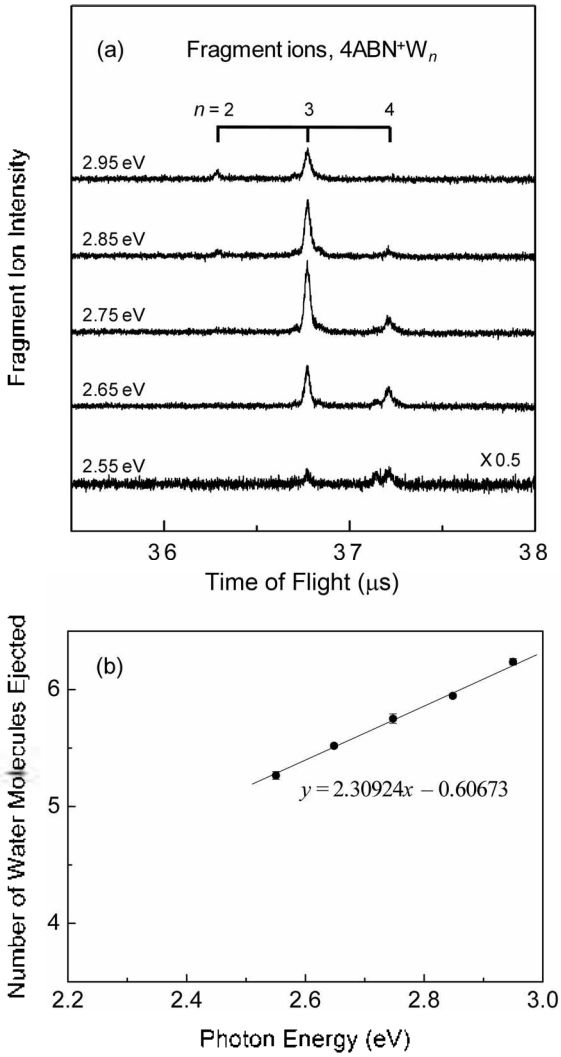

Figure 4. (a) Photofragmentation mass spectra (laser on-laser off) for $4ABN^-W_9$ at various photon energies. (b) The average number of ejected water molecules as a function of photon energy for $4ABN^-W_{18}$. The inverse of the slope represents the average binding of the water molecules.

$4ABN^+W_2$, $4ABN^-W_3$, and $4ABN_2^-$, respectively. Although we cannot completely rule out the effects of different rotational temperatures of each cluster on the shift mentioned above, it is thought that the shifts of LE band originate from the solvation effects. (Such shift was not observed at all when we employed different carrier gases for a given cluster ion.) It is gratifying that the blue shift is also expected from the TD-DFT (time-dependent density functional theory) calculation at the B3LYP/cc-pVDZ level; the excitation energies from the ground state to the excited state correspond to 2.6680 eV, 2.7283 eV, and 2.7500 eV for $4ABN^+W_1$, $4ABN^+W_2$, and $4ABN^-W_3$, respectively.

Photofragmentation mass spectra and binding energy. The photofragmentation mass spectra of the $4ABN^-W_9$ cluster (laser on-laser off) at various photon energies are shown in Figure 4(a). Figure 4(b) illustrates a linear dependence of the number of ejected water molecules over the photon energy ranging from 2.55 to 2.95 eV for $4ABN^-W_{18}$

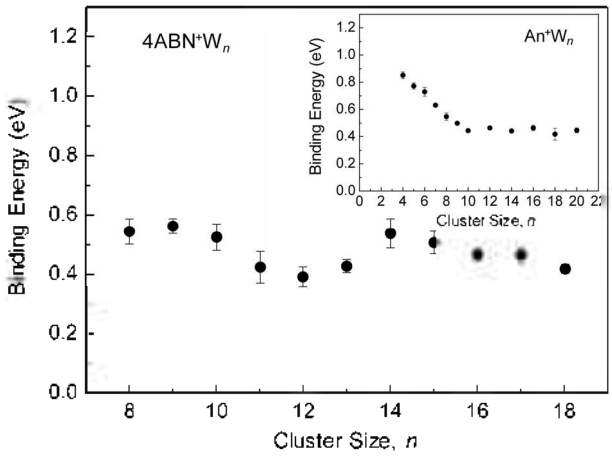

Figure 5. The average binding energy of the water molecules for $4ABN^-W_n$ (n = 8-18) *vs.* cluster size n. The inset indicates the average binding energy of the water molecules for An^-W_n (n = 4-20) *vs.* cluster size n.[11]

cluster, where the binding energy of the water molecule can be obtained from the inverse of the slope.[11] The binding energies for $4ABN^-W_n$ clusters (n = 8-18) are shown in Figure 5, which are close to those for An^-W_n clusters shown in the inset of Figure 5. The binding energy of water for $4ABN^-W_{18}$ cluster was 0.42 eV, which is close to the bulk vaporization energy of water. The binding energies for the smaller cluster ions ranged from 0.39 to 0.56 eV. In general, the binding energy of water molecule becomes smaller with increase in the size of the cluster because the effect of the "*ion core*" smears out. However, the binding energy increases from $4ABN^-W_{13}$ cluster, as shown in Figure 5, and gives a local maximum value for $4ABN^+W_{14}$ cluster. We can speculate that $4ABN^-W_{14}$ cluster forms a certain stable structure as in the case of An^+W_6 cluster.

Conclusion

The photodissociation dynamics of the $4ABN^-W_n$ (n = 8-18) clusters has been investigated to obtain the binding energies of water molecules, which ranged from 0.39 to 0.56 eV. The effects of cyano group on the binding energies turned out to be not significant. The LE bands of the $4ABN^-W_n$ (n = 1-3) clusters shifted gradually to the blue, which is in line with the results from TD-DFT calculation. According to the DFT calculation, it is predicted that the most stable structures of the $4ABN^+W_n$ clusters are quite close to those of the An^+W_n clusters, and the binding of water molecules at cyano site becomes less hindered energetically as the number of water molecules increases.

Acknowledgments. This work was funded by the Korea Research Foundation (KRF-2006-311-C00078).

References

1. Alexander, M. L.; Johnson, M. A.; Lineberger, W. C. *J. Chem. Phys.* **1985**, *82*, 5288.
2. Engelking, P. C. *J. Chem. Phys.* **1986**, *85*, 3103.

3. Ohashi, K.; Nishi, N. *J. Chem. Phys.* **1991**, *95*, 4002.
4. Beck, S. M.; Hecht, J. H. *J. Chem. Phys.* **1992**, *96*, 1975.
5. Ohashi, K.; Nakai, Y.; Shibata, T.; Nishi, N. *Laser Chem.* **1994**, *14*, 3.
6. Nakai, Y.; Ohashi, K.; Nishi, N. *J. Phys. Chem. A* **1997**, *101*, 472.
7. Ohashi, K.; Nishi, N. *J. Chem. Phys.* **1998**, *109*, 3971.
8. Inokuchi, Y.; Nishi, N. *J. Chem. Phys.* **2001**, *114*, 7059.
9. Watanabe, J.; Itakura, R.; Hishikawa, A.; Yamanouchi, K. *J. Chem. Phys.* **2002**, *116*, 9697.
10. Inokuchi, Y.; Ohashi, K.; Honokawa, Y.; Yamamoto, N.; Sekiya, H.; Nishi, N. *J. Phys. Chem. A* **2003**, *107*, 4230.
11. Nam, S. H.; Park, H. S.; Lee, M. A.; Cheong, N. R.; Song, J. K.; Park, S. M. *J. Chem. Phys.* **2007**, *126*, 224302.
12. Sakota, K.; Yamamoto, N.; Ohashi, K.; Sekiya, H.; Saeki, M.; Ishiuchi, S.; Sakai, M.; Fujii, M. *Chem. Phys. Lett.* **2001**, *341*, 70.
13. Sakota, K.; Yamamoto, N.; Ohashi, K.; Saeki, M.; Ishiuchi, S.; Sakai, M.; Fujii, M.; Sekiya, H. *Chem. Phys.* **2002**, *286*, 209.
14. Alejandro, E.; Fernández, J. A.; Castaño, F. *Chem. Phys. Lett.* **2002**, *353*, 195.
15. Sakota, K.; Yamamoto, N.; Ohashi, K.; Saeki, M.; Ishiuchi, S.; Sakai, M.; Fujii, M.; Sekiya, H. *Phys. Chem. Chem. Phys.* **2003**, *5*, 1775.
16. Gibson, E. M.; Jones, A. C.; Taylor, A. G; Bouwman, W. G; Phillips, D.; Sandell, J. *J. Phys. Chem.* **1988**, *92*, 5449.
17. Yu, H.; Joslin, E.; Crystall, B.; Smith, T.; Sinclair, W.; Phillips, D. *J. Phys. Chem.* **1993**, *97*, 8146.
18. Huang, L. C. L.; Lin, J. L.; Tzeng, W. B. *Chem. Phys.* **2000**, *261*, 449.
19. Borst, D. R.; Korter, T. M.; Pratt, D. W. *Chem. Phys. Lett.* **2001**, *350*, 485.
20. Jiang, S.; Levy, D. H. *J. Phys. Chem. A* **2002**, *106*, 8590.
21. Park, H. S.; Nam, S. H.; Song, J. K.; Park, S. M. *Int. J. Mass Spectrom.* **2007**, *262*, 73.
22. Nam, S. H.; Park, H. S.; Song, J. K.; Park, S. M. *J. Phys. Chem. A* **2007**, *111*, 3480.
23. Kappes, M. M.; Kunz, R. W.; Schumacher, E. *Chem. Phys. Lett.* **1982**, *91*, 413.